

Stiffness of Photocrosslinked RGD-Alginate Gels Regulates Adipose Progenitor Cell Behavior

Emily M. Chandler,¹ Caroline M. Berglund,² Jason S. Lee,¹ William J. Polacheck,² Jason P. Gleghorn,² Brian J. Kirby,² Claudia Fischbach¹

¹Department of Biomedical Engineering, Cornell University, Ithaca, New York; telephone: (607)-255-4547; fax: (607)-255-7330; e-mail: cf99@cornell.edu

²Sibley School of Mechanical & Aerospace Engineering, Cornell University, Ithaca, New York

Received 4 November 2010; revision received 17 January 2011; accepted 19 January 2011

Published online 15 February 2011 in Wiley Online Library (wileyonlinelibrary.com). DOI 10.1002/bit.23079

ABSTRACT: Adipose progenitor cells (APCs) are widely investigated for soft tissue reconstruction following tumor resection; however, the long-term success of current approaches is still limited. In order to develop clinically relevant therapies, a better understanding of the role of cell–microenvironment interactions in adipose tissue regeneration is essential. In particular, the effect of extracellular matrix (ECM) mechanics on the regenerative capability of APCs remains to be clarified. We have used artificial ECMs based on photocrosslinkable RGD-alginate to investigate the adipogenic and pro-angiogenic potential of 3T3-L1 preadipocytes as a function of matrix stiffness. These hydrogels allowed us to decouple matrix stiffness from changes in adhesion peptide density or extracellular Ca^{2+} concentration and provided a physiologically relevant 3D culture context. Our findings suggest that increased matrix rigidity promotes APC self-renewal and angiogenic capacity, whereas, it inhibits adipose differentiation. Collectively, this study advances our understanding of the role of ECM mechanics in adipose tissue formation and vascularization and will aid in the design of efficacious biomaterial scaffolds for adipose tissue engineering applications.

Biotechnol. Bioeng. 2011;108: 1683–1692.

© 2011 Wiley Periodicals, Inc.

KEYWORDS: alginate; mechanical stiffness; adipose progenitor cells; adipose tissue engineering; angiogenesis

Introduction

Adipose progenitor cells (APCs) are widely used for breast reconstruction following tumor resection (Patrick, 2000). In these applications, APCs are frequently transplanted on

biomaterial scaffolds and then used to stimulate soft tissue formation by both readily differentiating into adipocytes and through paracrine signaling with surrounding host cells (Parker and Katz, 2006). For example, APCs secrete pro-angiogenic factors (e.g., vascular endothelial growth factor; VEGF) that promote the recruitment of endothelial cells and angiogenesis (Lai et al., 2009; Rubina et al., 2009). New blood vessel formation, in turn, ensures the functionality of the newly developing adipose tissue by providing routes for endocrine and metabolic signaling (Gimeno and Klamann, 2005; Kershaw and Flier, 2004). While increasing experimental evidence indicates that cell–microenvironment interactions play a critical role in guiding adipogenesis (Fischbach et al., 2004; Stacey et al., 2009), the effect of dynamic changes of the extracellular matrix (ECM) mechanics on APC behavior remains largely unknown. This information is critical to the design of biomaterial scaffolds for adipose tissue engineering applications.

Changes in ECM rigidity broadly regulate cell behavior and may also impact the regenerative capabilities of APCs. ECM rigidity is largely controlled by the composition, cross-linking, and contraction of its protein components (Discher et al., 2005), and these parameters may vary locally at the site of APC implantation. Specifically, the mechanical properties of the ECM change during adipogenesis as the initially fibrillar ECM transforms into a laminar matrix structure (Mariman and Wang, 2010). Additionally, APCs may be exposed to pathologically enhanced ECM stiffness when they are located next to scars resulting from surgery (Corr et al., 2009) or tumors that may recur after resection (Samani et al., 2003). While matrix stiffness regulates the proliferation (Subramanian and Lin, 2005; Ulrich et al., 2009), differentiation (Engler et al., 2006), malignancy (Paszek et al., 2005), and angiogenesis (Mammoto et al., 2009) of various cell types, its specific effect on APC differentiation and pro-angiogenic activities is less well understood.

Matrices with adjustable mechanical but fixed chemical properties are necessary to study APC behavior in response to matrix stiffness. Frequently, MatrigelTM and collagen gels

Correspondence to: Claudia Fischbach

Contract grant sponsor: New York State Center for Advanced Technology

Contract grant sponsor: Morgan Tissue Engineering Fund

Contract grant sponsor: Cornell Center for Materials Research

Contract grant sponsor: National Science Foundation

Contract grant number: DMR 0520404

Contract grant sponsor: Graduate Research Fellowship for Emily Chandler

Additional Supporting Information may be found in the online version of this article.

of variable concentrations are used to evaluate the relationship between ECM mechanics and cell behavior (Karamichos et al., 2007; Zaman et al., 2006). However, this approach entails changes in adhesion ligand density, which regulates cellular functions independent of matrix stiffness (Boonthekul et al., 2008). Artificial ECMs may overcome these limitations by permitting decoupling of the physical and chemical matrix characteristics. Specifically, the rigidity of RGD-modified alginate hydrogels can be readily adjusted by ionic crosslinking with varying concentrations of Ca^{2+} (Kong et al., 2005). This approach, however, may not be suitable for studies of adipogenesis as it typically yields gels that are much stiffer than adipose tissue and because local concentrations of Ca^{2+} regulate APC functions (e.g., proliferation and differentiation (Boynton et al., 1974; Jensen et al., 2004)). Photocrosslinked, alginate-based hydrogels (Chou and Nicoll, 2009; Jeon et al., 2009; Rouillard et al., 2011; Smeds et al., 2001) may provide suitable alternatives to examine the effect of matrix stiffness on adipogenesis.

The goal of this study was to establish a biomaterial-based 3D culture system in order to evaluate the effect of matrix stiffness on the self-renewal, differentiation, and pro-angiogenic capacity of APCs under biologically relevant conditions. To this end, we have cultured 3T3-L1 preadipocytes, a well-established cell model for the study of adipogenesis (Ntambi and Young-Cheul, 2000), within photocrosslinked, RGD-modified alginate hydrogels that recreate tissue dimensionality and ECM mechanics representative of normal and pathological adipose tissue. Our results identify mechanical stiffness as an important regulator of APC function that must be considered in the design of efficacious and safe biomaterials for adipose tissue engineering.

Materials and Methods

Cell Culture

3T3-L1 cells (ATCC, Manassas, VA) were routinely cultured in MEM (α -modification, Sigma, St. Louis, MO) containing 10% fetal bovine serum (FBS, Tissue Culture Biologicals, Tulare, CA) and 1% antibiotic (penicillin/streptomycin; Gibco, Grand Island, NY). To induce adipogenesis, cells were maintained for 2 days in MEM (α -modification), 5% FBS, 1% antibiotic containing 1 μM insulin (Sigma), 100 nM corticosterone, 200 μM isobutylmethylxanthine, and 60 μM indomethacin (all from EMD, Gibbstown, NJ) as previously described (Fischbach et al., 2004). Subsequently, differentiation media [MEM (α -modification), 5% FBS, 1% antibiotic, and 1 μM insulin] was added, and cells were cultured under these conditions for 6 days, with media changes every other day.

Cell Viability in Response to Photocrosslinking Conditions

Cell viability in response to photocrosslinking conditions was tested in 2D culture by exposing 3T3-L1 cells to

increasing concentrations of VA-086 (Wako, Richmond, VA), Irgacure-2959 (Ciba, Basel, Switzerland), and varying durations of ultraviolet (UV) light (365 nm longwave, 2 $\mu\text{W}/\text{cm}^2$) in the absence of polymer. Specifically, cells were seeded into 12-well plates at equal densities and allowed to adhere overnight. Cultures were then treated with photoinitiators and/or UV light (using a Spectroline UV crosslinker) to simulate the conditions during hydrogel crosslinking. For these experiments, VA-086 and Irgacure-2959 were dissolved in water and 70% ethanol, respectively. Due to the different photoinitiator activities, 10-fold greater concentrations of VA-086 (0.1–0.4% w/v) were used as compared to Irgacure-2959 (0.01–0.04% w/v). Subsequently, dead cells were removed by rinsing the culture dishes with PBS, while adherent viable cells were trypsinized, and quantified using a Beckman Coulter counter.

Fabrication and Characterization of Photocrosslinked Alginate Hydrogels

Photocrosslinkable alginate was synthesized by reacting Protanal[®] LF10/60 (FMC Biopolymer, Philadelphia, PA) with methacrylic anhydride (Alfa Aesar, Ward Hill, MA), replacing secondary alcohols on the polymer with methacrylate groups (Fig. 1; Li et al., 2004; Rouillard et al., 2010; Smeds et al., 2001). To this end, methacrylic anhydride (Alfa Aesar) was added to a 2.5% w/v solution of alginate in deionized water while the pH was maintained with 5 M NaOH. After 72 h of reaction time, the alginate was washed with ethanol and filtered twice prior to lyophilization. In a second reaction, the obtained material was modified with GGGGRGDSP (Peptides International, Louisville, KY) adhesion peptides using standard carbodiimide chemistry as previously described (Rowley et al., 1999). To remove unreacted, low-molecular weight components, the alginate was purified by dialysis, and then the methacrylated RGD-alginate was sterile filtered and lyophilized. To prepare hydrogel disks for further analysis, a 3% (w/v) solution of methacrylated RGD-alginate in PBS was cast between two glass plates (separated by 1 mm spacers) and crosslinked in an UV crosslinker (Spectroline, Westburg, NY) for 5 min. The same modified polymer was used for all hydrogel systems; stiffness was altered by adjusting VA-086 concentrations to 0.1 (compliant gels), 0.2 (moderate gels), and 0.4 (stiff gels) % (w/v). Disks were punched out of the crosslinked slab of hydrogel using sterile biopsy punches ($d = 6$ mm). Aggregate moduli of photocrosslinked alginate were measured under radial confinement and uniaxial compression using a mechanical tester (ELF 3100; Bose, Eden Prairie, MN). Alginate hydrogels were incrementally loaded at steps of 5% compression with the reported aggregate modulus measured from the slope fit to the stress-strain curve at 15% strain. To ensure that gel modulus was maintained through experiments, the aggregate moduli of different batches were measured. Additionally, for experiments where direct comparisons were made between conditions, the same batch of material was used. To ensure

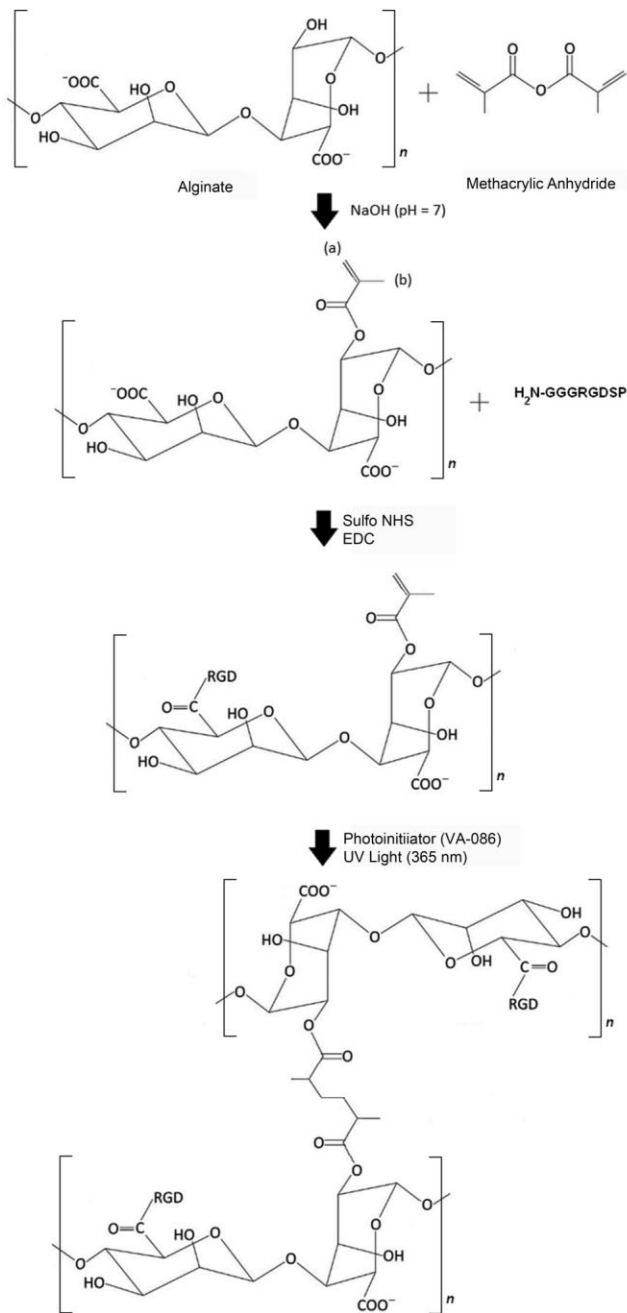


Figure 1. Development of photocrosslinked RGD-alginate hydrogels. Methacrylated alginate was synthesized by reaction of LF10/60 alginate with methacrylic anhydride and was subsequently modified with RGD-adhesion peptides using carbodiimide chemistry. Exposure of the resulting material to UV light in the presence of a photoinitiator yielded photocrosslinked RGD-alginate hydrogels.

maintenance of gel mechanical character for the duration of the culture experiments, the aggregate modulus of compliant alginate gels was measured in the same manner as described above over a period of 2 weeks. Gel swelling was assessed by measuring the wet and dry weights of alginate gels, pre- and post-lyophilization, respectively, over a 6-week period. To encapsulate 3T3-L1, into 3D hydrogels, cells were suspended in the alginate solution prior to gelation at a

concentration of 1.5×10^6 cells/mL. The resulting matrices were subsequently cultured under dynamic conditions on a Bellco orbital shaker. The day of cell encapsulation was considered day 0.

Analysis of Cell Adhesion and Proliferation

Cell adhesion was measured under 2D conditions. 3T3-L1 preadipocytes were seeded onto non-modified and RGD-modified alginate disks of equal aggregate modulus (~ 12 kPa). After 16 h of culture, cells were fixed and stained with Alexa Fluor 568 phalloidin (Invitrogen, Carlsbad, CA, 1:100) and DAPI (Invitrogen, 1:5,000). The cells were visualized using a fluorescent microscope (Zeiss Observer Z.1), and three representative images per gel were taken with an AxioCam MRN camera. Cell spreading was quantified via image analysis (ImageJ, NIH) by measuring the average surface area per cell for three gels per condition.

Cell proliferation was tested under 3D conditions. Cells were released from their matrices by dissolution of the gels in a solution of alginate lyase (3.3 units/g alginate, Sigma) in PBS on days 0, 3, and 7. Cell numbers in the resulting cell suspension were determined with a Beckman coulter counter. Additionally, cell-encapsulating alginate disks were subjected to live/dead staining using calcein (Invitrogen, $1 \mu\text{g/mL}$ for 15 min) and propidium iodide (Sigma, $10 \mu\text{g/mL}$ for 5 min), respectively. Eight representative images of three gels per condition were taken at randomly selected locations on each gel for viability quantification via image analysis.

Analysis of Adipose Differentiation

Differentiated cells were harvested from their 3D matrices by alginate lyase treatment as described above. The resulting cell pellet was lysed on ice in a buffer containing 50 mM Tris, 1 mM EDTA, and 1 mM β -mercaptoethanol (all from J.T. Baker, Phillipsburg, NJ). Subsequently, glycerol-3-phosphate dehydrogenase (GPDH) activity was measured using a spectrophotometer as previously reported (Fischbach et al., 2004). Briefly, supernatants obtained from the lysates were mixed with dihydroxyacetone phosphate and the oxidized form of nicotinamide adenine dinucleotide (NADH). GPDH activity was assessed by quantifying the decrease in NADH absorbance at 340 nm over a 7-min period. Enzyme activity was normalized to total protein content as measured by the Bio-Rad Protein assay per manufacturer's protocol. To visualize lipid accumulation, cell-incorporating gels were fixed overnight in formalin, stained with Oil Red O (Sigma, 0.3% w/v solution in 60% isopropyl alcohol) for 2 h, and then interrogated with bright field microscopy.

Analysis of VEGF Secretion

On day 3, cell-incorporating hydrogel disks were transferred to new culture dishes containing MEM (α -modification)

with 1% FBS and 1% antibiotic. Media were collected after 24 h and analyzed for VEGF via Quantikine ELISA (R&D, Minneapolis, MN). To additionally determine the amount of matrix-sequestered VEGF, alginate constructs were dissolved with alginate lyase as described above and the VEGF content of the resulting solution was measured. Prior studies verified that alginate lyase treatment does not compromise VEGF analysis as incubation of recombinant VEGF with alginate lyase and subsequent ELISA yielded similar VEGF concentrations as samples not exposed to alginate lyase (Supplementary Fig. 1). Indicated values represent the total amount of VEGF quantified in the conditioned media as well as the gel lysate. VEGF data were normalized to cell number as determined at the time of media harvest to account for cell proliferation differences between conditions.

Analysis of Endothelial Cell Behavior

Human umbilical vein endothelial cells (HUVECs; Lonza, Walkersville, MD) were routinely cultured in endothelial growth medium (EGM-2, Lonza). 3T3-L1-conditioned media was collected as described above for VEGF analysis, concentrated twofold using Amicon centrifugal filter units (Millipore, Billerica, MA, MWCO = 3 kDa), and subsequently reconstituted with EGM-2 from which growth factors were omitted. HUVEC proliferation was assessed by cell counting after 5 days of culture in reconstituted conditioned media. To assess cord formation, HUVECs were seeded onto Matrigel™ (BD, Franklin Lakes, NJ) in conditioned media. After 24 h, the cells were stained with calcein (Invitrogen, 1 μg/mL) and imaged on a Zeiss Observer Z.1 microscope using an AxioCam MRN camera. Three randomly selected areas were imaged and analyzed per well with three wells per condition. The connectivity and length of the tubular structures were assessed using a MATLAB®-based program (AngioQuant; Niemisto et al., 2005).

Statistical Analysis

All data are reported as means ± standard deviations and were analyzed by one-way analysis of variance (ANOVA) followed by the Newman-Keuls method to make post hoc pair wise comparisons using Prism 5 (GraphPad Software) with $\alpha = 0.05$ (* $P < 0.05$; ** $P < 0.01$ between noted conditions).

Results

Establishment of Photocrosslinking Conditions

To enable cytocompatible photocrosslinking, we initially tested the effect of two widely used photoinitiators, Irgacure-2959 and VA-086 (Jeon et al., 2009; Rouillard

et al., 2010), on 3T3-L1 viability. For these experiments, relevant concentrations of these two substances were added to the media of standard 2D cell cultures (i.e., in the absence of the polymer). Our results indicated that VA-086 in 10-fold higher mass concentration is less toxic to 3T3-L1 cells than Irgacure-2959 (Fig. 2a and b), both with and without UV exposure. Specifically, 0.04% Irgacure-2959 in conjunction with 15 min UV [i.e., conditions necessary to produce the stiff gels (see below)] dramatically decreased cell viability to 2% (Fig. 2a). In contrast, exposure to 0.4% VA-086 and 5 min UV [i.e., conditions needed to produce similarly stiff gels (see below)] resulted in 82% viability. To assess whether these differences were due to the varying UV exposure times we additionally irradiated cultures with VA-086 for 15 min. In these experiments, cell viability was slightly reduced as compared to treatment for 5 min, but still remained at 77% for the highest VA-086 concentration (Fig. 2b). The reduced viability in the 0% Irgacure-2959 condition relative to the 0% VA-086 condition after 15 min of UV may be caused by the different solvents (ethanol

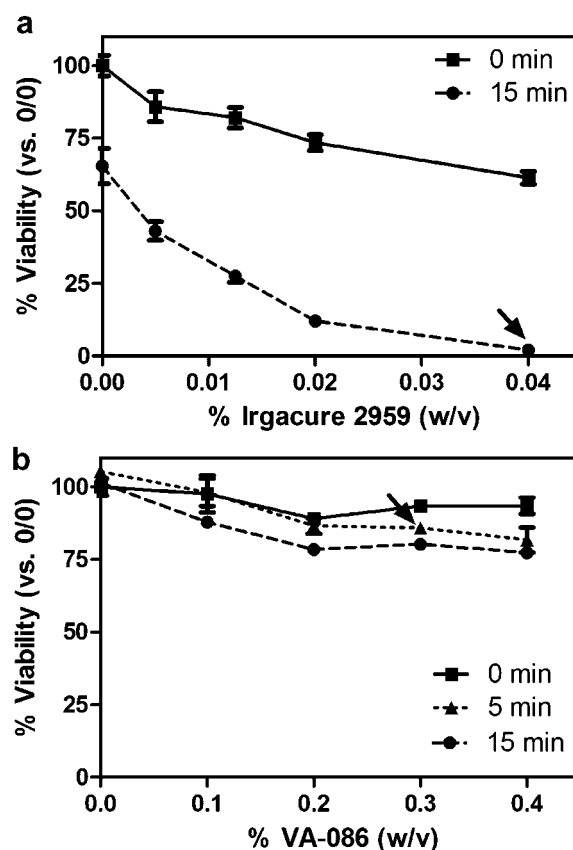


Figure 2. Cell viability in response to photocrosslinking conditions. Control experiments in 2D cell culture indicate that 3T3-L1 viability is lower following photocrosslinking with Irgacure-2959 (a) compared with VA-086 (b). The percentage of viable cells is expressed relative to control conditions in which cells were neither treated with photoinitiator nor exposed to UV light (0/0); however, an equal volume of the solvent (water or 70% ethanol for VA-086 or Irgacure-2959, respectively), was added to the control condition. Arrows indicate photocrosslinking conditions that would be necessary to produce gels with a modulus of 12 kPa (stiff condition).

for Irgacure-2959, water for VA-086). Nevertheless, the different solvents do not account for the observed changes in cell viability in the presence of photoinitiators because VA-086 is also less cytotoxic than Irgacure-2959 when dissolved in ethanol (Rouillard et al., 2011). Collectively, treatment with VA-086 (0.4%; 5 min UV) yields 41-fold enhanced 3T3-L1 cell numbers as compared to Irgacure-2959 (0.04%; 15 min UV) and was, therefore, used for all experiments involving photocrosslinking of cell-incorporating alginate matrices.

Development of Artificial ECMs With Relevant Matrix Stiffnesses

Next, we tested our ability to generate 3D hydrogel matrices of biologically relevant stiffness by photocrosslinking

methacrylated alginate with VA-086. The crosslinking density of the gels was adjusted by altering the concentration of the photoinitiator VA-086. Mechanical testing confirmed that the elastic moduli of the resulting matrices were 3.3, 7.9, and 12.4 kPa and, therefore, representative of physiological (~ 2 kPa), intermediate, and pathological (~ 12 kPa) stiffness ranges detected, for example, during tumorigenesis (Samani et al., 2003; Fig. 3a). These moduli were maintained throughout the time of 3D culture, as no significant changes were detected over 2 weeks (Fig. 3b). Additionally, measurement of gel wet and dry weight indicated no significant swelling during the duration of the experiment that would otherwise alter the mechanical characteristics of the gels (Fig. 3c).

Subsequently, we modified the photocrosslinkable alginate by covalent coupling of adhesive RGD peptides

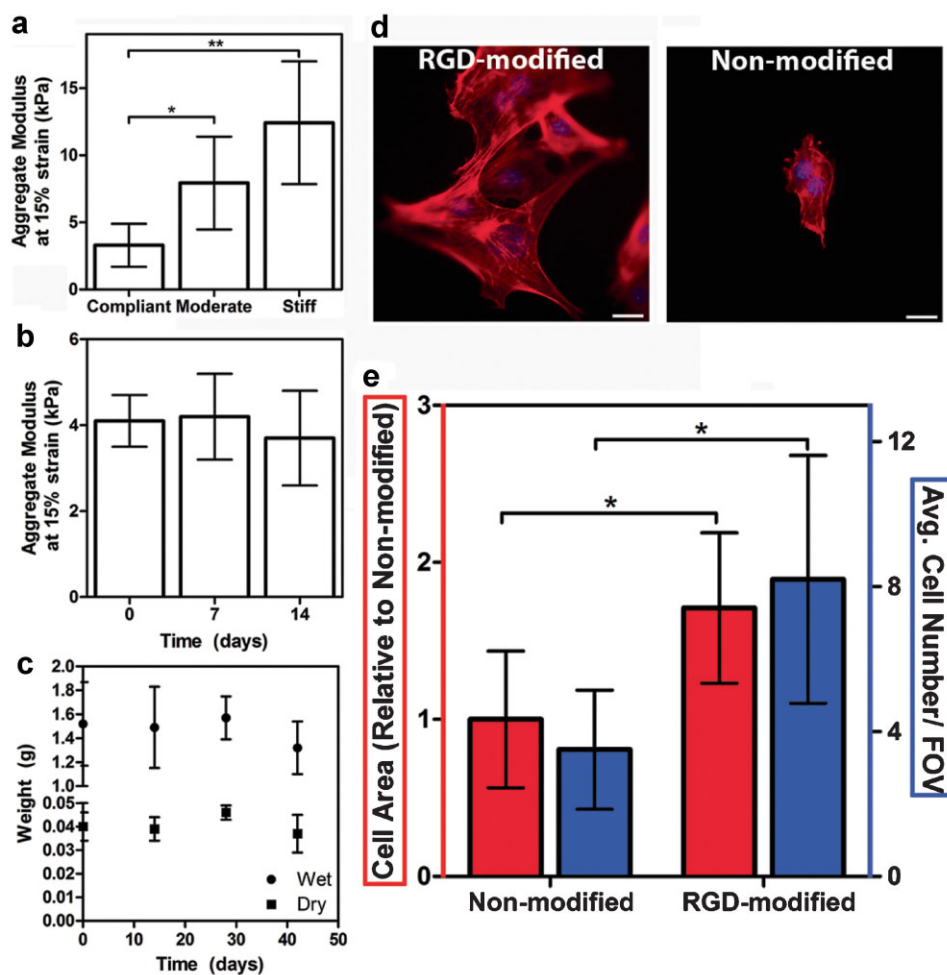


Figure 3. Characterization of the developed materials. Mechanical testing verified that gels that mimicked moduli of normal (compliant), intermediate (moderate), and pathological (stiff) adipose tissue could be engineered by controlling photoinitiator concentration (a, $n = 5$ or 6) and that the modulus did not change significantly during the culture time period (b, $n = 4$). No significant swelling in the gels was seen after initial equilibration as the wet and dry weights of the alginate gels were maintained for periods longer than the duration of the experiments (c, $n = 3$). Covalent modification of methacrylated alginate with RGD adhesion peptides promoted 3T3-L1 adhesion and spreading on 2D hydrogel disks. Fluorescent staining was performed with DAPI and phalloidin to visualize actin (red) and nuclei (blue), respectively. Scale bars represent $20 \mu\text{m}$ (d). Average cell area and number of adhered cells per field of view (FOV) were quantified by analyzing the images (e, $n = 3$). (* $P < 0.05$; ** $P < 0.01$). [Color figure can be seen in the online version of this article, available at <http://wileyonlinelibrary.com/bit>]

according to a previously established protocol (Fig. 1; Rowley et al., 1999). This reaction resulted in the introduction of two cellular binding sites per alginate chain (Lee et al., 2004) and enabled integrin engagement necessary for cells to sense changes in matrix stiffness (Wang et al., 1993). Successful RGD modification was confirmed with a simple 2D adhesion assay in which cells were seeded on top of hydrogel disks with aggregate modulus of 12 kPa. 3T3-L1 cells readily adhered and spread on RGD-modified alginate, whereas cell adhesion was dramatically reduced on non-modified alginate (Fig. 3d). Specifically, both cell numbers and cell surface areas were significantly increased on RGD-modified disks relative to non-modified cultures (Fig. 3e).

3T3-L1 Proliferation and Viability Within Hydrogels With Different Modulus

We determined 3T3-L1 number and viability within the 3D hydrogel matrices to assess the effect of mechanical stiffness on APC self-renewal. The number of 3T3-L1 cells within 7.9 kPa (moderate) and 12.4 kPa (stiff) hydrogels increased over time, while no significant change was detected in 3.3 kPa (compliant) matrices (Fig. 4a). At day 0, cellularity was similar for all conditions, suggesting that the detected differences were due to changes in cell proliferation rather

than encapsulation efficiency. Live/dead staining after 7 days in culture, furthermore, indicated that culture within compliant gels promoted cell death as compared to culture within moderate and stiff gels. The resulting changes in cell viability likely contributed to the detected variations in cell number by mediating a decrease in the population of proliferative cells (Fig. 4b and c).

3T3-L1 Differentiation Within Hydrogels of Varying Stiffness

To evaluate the effect of matrix stiffness on adipogenesis, typical markers of lipid biosynthesis were analyzed following 8 days of differentiation. GPDH activity, a key enzyme involved in lipid accumulation, decreased with increasing ECM stiffness (Fig. 5). Specifically, 3T3-L1 cells that differentiated within stiff gels exhibited 1.4-fold and 2.4-fold reduced GPDH activity relative to the same cells maintained within moderate and compliant gels, respectively (Fig. 5a). Visualization of lipid biosynthesis via Oil Red O staining further confirmed that cells in compliant matrices produced enlarged fat droplets as compared to cells cultured within the stiffer matrices (Fig. 5b). Because 3T3-L1 differentiation was induced immediately after seeding, no proliferation phase occurred and these results cannot be attributed to changes in cell numbers due to

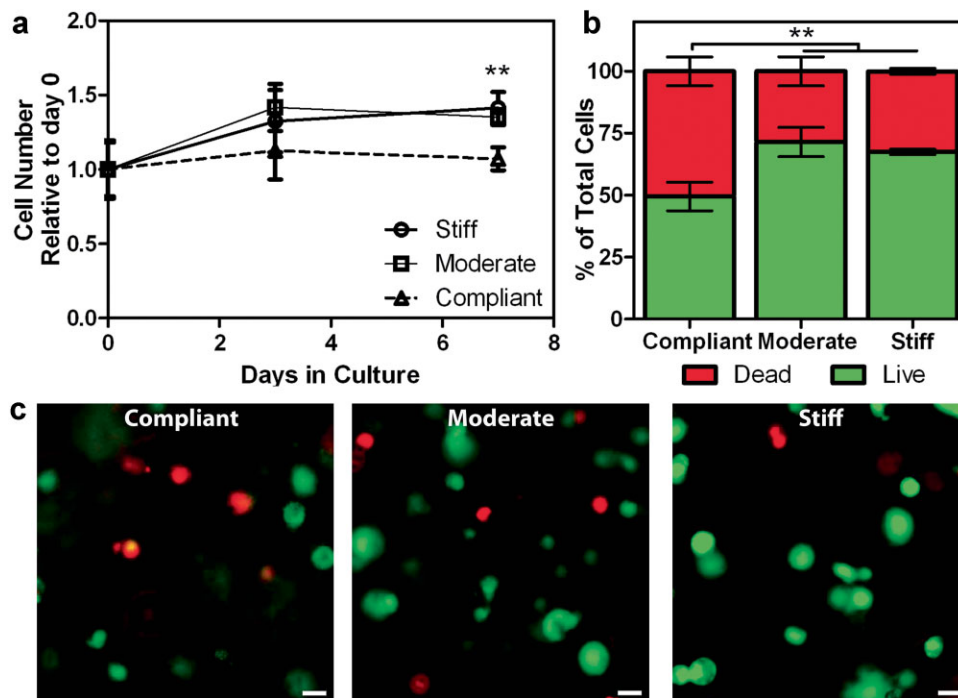


Figure 4. Proliferation and viability within 3D hydrogel cultures. Significantly more 3T3-L1 cells were observed following culture within the stiff and moderately stiff gels compared with the compliant gels (a, $n = 4$). At day 7, cell viability in the stiff and moderate gels was higher relative to the compliant gels as assessed by image analysis (b, $n = 4$) of live and dead cells following staining with calcein (green) and propidium iodide (red), respectively. Scale bars represent 20 μm (c). (** $P < 0.01$).

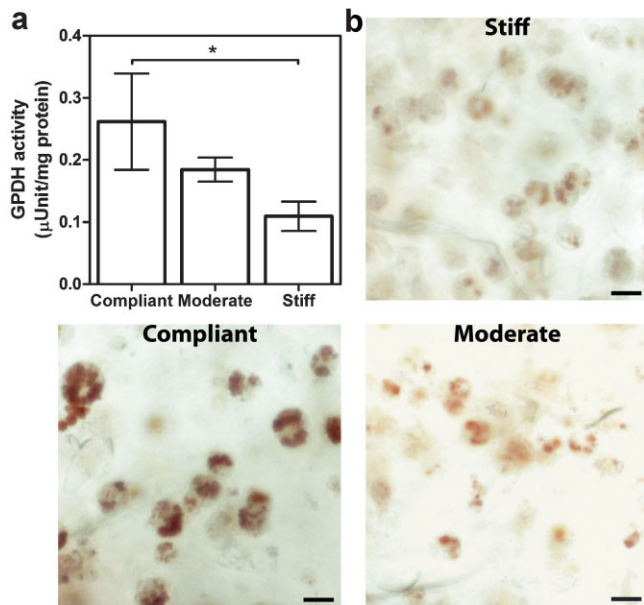


Figure 5. Adipose differentiation within 3D hydrogel cultures. Differentiation of 3T3-L1 cells into adipocytes was higher within compliant gels relative to stiffer gels as determined by analysis of GPDH activity (a, $n = 4$) and microscopic evaluation of lipid droplet size following Oil Red O staining 1 week after inducing differentiation. Scale bars represent 20 μm (b). ($*P < 0.05$). [Color figure can be seen in the online version of this article, available at <http://wileyonlinelibrary.com/bit>]

altered proliferation. Consequently, our data suggest that adipose differentiation of 3T3-L1 cells is inhibited in stiff matrices and that a combination of chemical and mechanical cues contributed to this as no adipogenesis was observed in the absence of hormonal induction.

Pro-Angiogenic Capacity of 3T3-L1 in Response to Varying Stiffness

We analyzed VEGF secretion of 3T3-L1 preadipocytes in the different hydrogels to assess the effect of 3D matrix stiffness on the pro-angiogenic potential of these cells. 3T3-L1s cultured within stiff gels secreted significantly more VEGF as compared to the same cells contained within compliant gels (Fig. 6a). No significant difference in VEGF secretion was detected between the compliant and moderate culture systems. The observed effects can be attributed to changes in secretion rather than variable sequestration within the different matrices, because similar amounts of VEGF were retained in compliant ($45 \pm 13\%$ of total VEGF) and stiff gels ($47 \pm 5\%$ of total VEGF). In these experiments, VEGF secretion was normalized to cell number at the time of harvest, thus the differences indicate altered secretion and not differences in cell number. To evaluate the physiologic relevance of these changes, we analyzed HUVEC behavior in response to media collected from the different substrates. Media conditioned by 3T3-L1 cells in stiff matrices promoted HUVEC proliferation (Fig. 6b) and tube formation on MatrigelTM (Fig. 6c and d) as compared

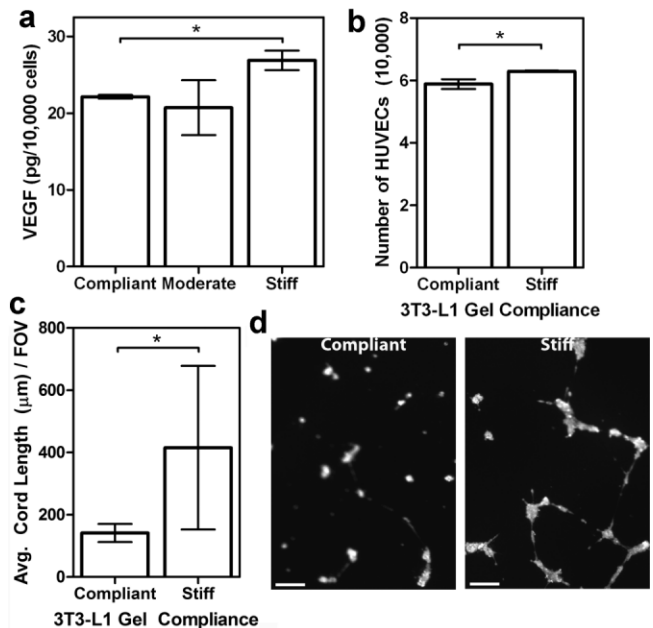


Figure 6. Pro-angiogenic potential of 3T3-L1 in 3D hydrogel cultures. 3T3-L1 cells cultured within stiff hydrogel matrices secreted larger concentrations of VEGF normalized to cell number compared with those maintained within more compliant gels (a, $n = 4$). Conditioned media collected from cells maintained in stiffer matrices enhanced HUVEC proliferation (b, $n = 4$) and capillary tube formation on Matrigel [c($n = 3$)] (d) relative to media obtained from compliant cultures. Scale bars represent 50 μm . ($*P < 0.05$).

to media collected from cells within compliant substrates. Additionally, conditioned media from stiff cultures promoted transwell migration of endothelial cells (305 ± 24 HUVECs/FOV) relative to media from compliant cultures (286 ± 34 HUVECs/FOV).

Discussion

We have characterized a biologically relevant 3D culture system for 3T3-L1 cells and used it to evaluate the effect of matrix stiffness on the self-renewal, differentiation, and pro-angiogenic capacity of APCs. This model system is based on photocrosslinked RGD-modified alginate and through its use, we decoupled matrix stiffness from changes in adhesion peptide density or extracellular Ca^{2+} concentration, which may independently affect APC behavior (Boonthekul et al., 2008; Boynton et al., 1974; Jensen et al., 2004). Our data indicate that enhanced matrix rigidity significantly decreases adipose differentiation of APCs, whereas it increases the number and angiogenic capacity of these cells. Collectively, our results define matrix stiffness as an important design parameter for the development of biomaterial scaffolds for adipose tissue engineering.

Methacrylation of natural and synthetic polymers and subsequent photocrosslinking with Irgacure-2959 is widely used to prepare hydrogels for tissue engineering

applications. For example, chitosan (Ono et al., 2000), hyaluronic acid (Baier Leach et al., 2003), and poly(ethylene glycol) (PEG; Sawhney et al., 1993) based gels have been developed with this approach, and, more recently, similar techniques have been used to generate photocrosslinked alginate gels (Jeon et al., 2009; Rouillard et al., 2011; Smeds et al., 2001). However, alginate lacks integrin engagement sites that are necessary for cells to sense mechanical stiffness (Matthews et al., 2006). Consequently, photocrosslinked alginate gels without adhesion peptides do not permit studies of APC behavior as a function of 3D matrix rigidity. To address this challenge, we have developed a protocol that involves RGD modification of methacrylated alginate, similar to a recently published method (Jeon et al., 2010). Additionally, we have systematically tested different photoinitiators for the crosslinking of these materials. While Irgacure-2959 is frequently used for a wide range of cell types [e.g., chondrocytes (Jeon et al., 2009), endothelial cells (Baier Leach et al., 2003), and hepatocytes (Underhill et al., 2007)], we here show that VA-086 may be more suitable for 3D cell encapsulation of 3T3-L1s as it maintains cell viability to a greater extent than Irgacure-2959, similar to studies with chondrocytes (Rouillard et al., 2011). Our conclusions are based on 2D experiments in which the photoinitiators were added to the culture media rather than mixed into a cell-polymer solution. While methacrylated monomers can protect cells from protein denaturation and DNA damage by high-energy free radicals (Lin et al., 2008), cytotoxicity results in 2D culture have been shown to qualitatively parallel 3D cultures in chondrocyte constructs (Rouillard et al., 2011).

We used the developed RGD-alginate gels to study APC behavior in response to varying stiffnesses under 3D culture conditions. Previous studies have indicated that matrix elasticity regulates the proliferation and differentiation capacity of stem cells on 2D substrates (Engler et al., 2006; Subramanian and Lin, 2005; Ulrich et al., 2009), and that compliant matrices may be a prerequisite for adipose differentiation in 2D culture (Winer et al., 2009). However, integrin mechanoreceptors may signal differently in 2D and 3D culture (Cukierman et al., 2001), and we, therefore, aimed at investigating APC behavior under 3D conditions. Our results suggest that, according to previous 2D studies, adipose differentiation is greatest in matrices with a modulus that is similar to adipose tissue, whereas, less compliant substrates inhibit this process and increase the proliferative and angiogenic potential of APCs. These differences may be related to adhesion-dependent changes in cell contractility. In particular, cells encapsulated in stiff matrices exhibit increased integrin engagement, cell proliferation, and angiogenic factor expression as compared to those in compliant matrices (Discher et al., 2005; Seib et al., 2009), and changes in cytoskeletal tension and intracellular signaling may contribute to this (McBeath et al., 2004; Pirone et al., 2006). In contrast, adipose differentiation is favored in softer environments with which cells interact less strongly and consequentially undergo morphological

changes that favor adipogenesis (McBeath et al., 2004). Future studies using pharmacological inhibition of the associated signaling pathways will help to probe these connections.

Vascularization of adipose tissue is mediated by a concerted and complex interplay between multiple pro- and anti-angiogenic factors. For example, VEGF dynamically interacts with basic fibroblast growth factor (bFGF) and interleukin-8 (IL-8; Yoshida et al., 1997) to activate endothelial cell proliferation and migration that leads to the formation of new blood vessels, while anti-angiogenic factors such as thrombospondin inhibit these processes (Taraboletti et al., 1990). To the best of our knowledge, our studies for the first time suggest that mechanical stiffness results in the up-regulation of VEGF in APCs. Nevertheless, the detected differences in VEGF secretion may only partially account for the significant increase in tube formation observed on MatrigelTM. It is likely that a stiffness-mediated increase of other pro-angiogenic molecules, or downregulation of anti-angiogenic factors, contributes to the detected angiogenic effects in our experiments; this deserves future study.

The reported results have important implications for the design of biomaterial scaffolds for adipose tissue engineering. Successful adipose tissue engineering approaches rely on both adipose differentiation and the rapid recruitment of a vascular network to meet the metabolic requirements of the newly formed fat pad (Patrick, 2000). It may be possible to satisfy these biological design parameters by the development of hydrogel composites that consist of spatially defined compliant and stiff compartments that drive adipose tissue regeneration by promoting adipogenesis and pro-angiogenic factor secretion, respectively. Such polymeric systems would be particularly useful when combined with endothelial cells (Kang et al., 2009). Specifically, our results indicate that co-implanted endothelial cells may be able to accelerate vascularization by increased proliferation and tube formation in response to the elevated concentration of pro-angiogenic factors (e.g., VEGF) from APCs. In contrast, implantation of APCs within matrices exhibiting stiffnesses >10 kPa may not result in efficacious and safe therapies, as the encapsulated cells may undergo very limited differentiation into adipocytes, while potentially promoting pathological angiogenesis. In particular, enhanced concentrations of pro-angiogenic factors can activate the angiogenic switch in dormant tumors (Naumov et al., 2006), which is critical to tumor induction, progression, and metastasis. This process may be further enhanced because increased matrix rigidity promotes blood vessel formation by directly altering endothelial cell behavior (Mammoto et al., 2009). This possible perturbation of blood vessel homeostasis represents a particularly important problem, as adipose tissue engineering is predominantly pursued for reconstruction therapies for breast cancer patients who carry the risk of tumor recurrence (Patrick, 2000).

While the focus of this study was to investigate the role of mechanical stiffness on APC proliferation, adipose

differentiation, and pro-angiogenic capability in a 3D culture context, a number of related questions could also be studied with the developed hydrogels. For example, does mechanical stiffness also influence the behavior of fully differentiated adipocytes? What happens if APCs are not exposed to differential mechanical environments until after they are hormonally induced to undergo differentiation? Would they still respond differently to soft and stiff matrices? Finally, APCs are multipotent and have been shown to differentiate into other lineages including chondrocytes, osteoblasts, and endothelial cells (Gimble et al., 2007). To what extent are mechanical cues involved in guiding these cells along a specific lineage? The materials described in this study provide an important platform that can be used to address all of these questions. As the developed photocrosslinkable materials can be processed into 2D and 3D substrates, they may also be useful to assess differences as a function of tissue dimensionality.

Conclusions

We explored RGD-functionalized, photocrosslinkable alginate gels to evaluate the effect of ECM mechanics on APC behavior under physiologically relevant 3D culture conditions. Using these model systems, we revealed that increased ECM stiffness inhibits adipose differentiation, while increasing the proliferative and angiogenic potential of these cells. Based on these observations, it may be possible to enhance adipose regeneration by implanting APCs in composite hydrogels that consist of both compliant and stiff compartments. Our results suggest that this approach might simultaneously promote adipogenesis and angiogenesis, two processes critical to the long-term success of engineered adipose tissue. In total, our results provide an improved understanding of the role of ECM stiffness in adipose tissue regeneration, and inform adipose tissue engineering approaches.

The authors would like to thank Dr. Lawrence Bonassar for use of equipment and for helpful discussions and Weilin Yang for help with swelling data collection. Funding was provided by an innovation grant of the New York State Center for Advanced Technology, the Morgan Tissue Engineering grant, the Cornell Center for Materials Research, and the National Science Foundation (DMR 0520404 and a Graduate Research Fellowship for Emily Chandler).

References

Baier Leach J, Bivens KA, Patrick CW, Jr, Schmidt CE. 2003. Photocrosslinked hyaluronic acid hydrogels: Natural, biodegradable tissue engineering scaffolds. *Biotechnol Bioeng* 82(5):578–589.

Boonthekul T, Kong HJ, Hsiong SX, Huang YC, Mahadevan L, Vandenburgh H, Mooney DJ. 2008. Quantifying the relation between bond number and myoblast proliferation. *Faraday Discuss* 139:53–70. discussion 105–128, 419–420.

Boynton AL, Whitfield JF, Isaacs RJ, Morton HJ. 1974. Control of 3T3 cell proliferation by calcium. *In Vitro* 10:12–17.

Chou AI, Nicoll SB. 2009. Characterization of photocrosslinked alginate hydrogels for nucleus pulposus cell encapsulation. *J Biomed Mater Res A* 91(1):187–194.

Corr DT, Gallant-Behm CL, Shrive NG, Hart DA. 2009. Biomechanical behavior of scar tissue and uninjured skin in a porcine model. *Wound Repair Regen* 17(2):250–259.

Cukierman E, Pankov R, Stevens DR, Yamada KM. 2001. Taking cell-matrix adhesions to the third dimension. *Science* 294(5547):1708–1712.

Discher DE, Janmey P, Wang YL. 2005. Tissue cells feel and respond to the stiffness of their substrate. *Science* 310(5751):1139–1143.

Engler AJ, Sen S, Sweeney HL, Discher DE. 2006. Matrix elasticity directs stem cell lineage specification. *Cell* 126(4):677–689.

Fischbach C, Spruss T, Weiser B, Neubauer M, Becker C, Hacker M, Gopferich A, Blunk T. 2004. Generation of mature fat pads in vitro and in vivo utilizing 3-D long-term culture of 3T3-L1 preadipocytes. *Exp Cell Res* 300(1):54–64.

Gimble JM, Katz AJ, Bunnell BA. 2007. Adipose-derived stem cells for regenerative medicine. *Circ Res* 100(9):1249–1260.

Gimeno RE, Klamann LD. 2005. Adipose tissue as an active endocrine organ: Recent advances. *Curr Opin Pharmacol* 5(2):122–128.

Jensen B, Farach-Carson MC, Kenaley E, Akanbi KA. 2004. High extracellular calcium attenuates adipogenesis in 3T3-L1 preadipocytes. *Exp Cell Res* 301(2):280–292.

Jeon O, Bouhadir KH, Mansour JM, Alsborg E. 2009. Photocrosslinked alginate hydrogels with tunable biodegradation rates and mechanical properties. *Biomaterials* 30(14):2724–2734.

Jeon O, Powell C, Ahmed SM, Alsborg E. 2010. Biodegradable, photocrosslinked alginate hydrogels with independently tailorable physical properties and cell adhesivity. *Tissue Eng Part A* 16(9):2915–2925.

Kang JH, Gimble JM, Kaplan DL. 2009. In vitro 3D model for human vascularized adipose tissue. *Tissue Eng Part A* 15(8):2227–2236.

Karamichos D, Brown RA, Mudera V. 2007. Collagen stiffness regulates cellular contraction and matrix remodeling gene expression. *J Biomed Mater Res Part A* 83A(3):887–894.

Kershaw EE, Flier JS. 2004. Adipose tissue as an endocrine organ. *J Clin Endocrinol Metab* 89(6):2548–2556.

Kong HJ, Liu J, Riddle K, Matsumoto T, Leach K, Mooney DJ. 2005. Non-viral gene delivery regulated by stiffness of cell adhesion substrates. *Nat Mater* 4(6):460–464.

Lai N, Jayaraman A, Lee K. 2009. Enhanced proliferation of human umbilical vein endothelial cells and differentiation of 3T3-L1 adipocytes in coculture. *Tissue Eng Part A* 15(5):1053–1061.

Lee KY, Alsborg E, Hsiong S, Comisar W, Linderman J, Ziff R, Mooney D. 2004. Nanoscale adhesion ligand organization regulates osteoblast proliferation and differentiation. *Nano Lett* 4(8):1501–1506.

Li Q, Williams CG, Sun DD, Wang J, Leong K, Elisseeff JH. 2004. Photocrosslinkable polysaccharides based on chondroitin sulfate. *J Biomed Mater Res A* 68(1):28–33.

Lin CC, Sawicki SM, Metters AT. 2008. Free-radical-mediated protein inactivation and recovery during protein photoencapsulation. *Biomacromolecules* 9(1):75–83.

Mammoto A, Connor KM, Mammoto T, Yung CW, Huh D, Aderman CM, Mostoslavsky G, Smith LE, Ingber DE. 2009. A mechanosensitive transcriptional mechanism that controls angiogenesis. *Nature* 457(7233):1103–1108.

Mariman EC, Wang P. 2010. Adipocyte extracellular matrix composition, dynamics and role in obesity. *Cell Mol Life Sci* 67(8):1277–1292.

Matthews BD, Overby DR, Mannix R, Ingber DE. 2006. Cellular adaptation to mechanical stress: Role of integrins, Rho, cytoskeletal tension and mechanosensitive ion channels. *J Cell Sci* 119(Pt 3):508–518.

McBeath R, Pirone DM, Nelson CM, Bhadriraju K, Chen CS. 2004. Cell shape, cytoskeletal tension, and RhoA regulate stem cell lineage commitment. *Dev Cell* 6(4):483–495.

Naumov GN, Akslen LA, Folkman J. 2006. Role of angiogenesis in human tumor dormancy: Animal models of the angiogenic switch. *Cell Cycle* 5(16):1779–1787.

- Niemisto A, Dunmire V, Yli-Harja O, Zhang W, Shmulevich I. 2005. Robust quantification of in vitro angiogenesis through image analysis. *IEEE Trans Med Imaging* 24(4):549–553.
- Ntambi JM, Young-Cheul K. 2000. Adipocyte differentiation and gene expression. *J Nutr* 130(12):3122S–3126S.
- Ono K, Saito Y, Yura H, Ishikawa K, Kurita A, Akaike T, Ishihara M. 2000. Photocrosslinkable chitosan as a biological adhesive. *J Biomed Mater Res* 49(2):289–295.
- Parker AM, Katz AJ. 2006. Adipose-derived stem cells for the regeneration of damaged tissues. *Expert Opin Biol Ther* 6(6):567–578.
- Paszek MJ, Zahir N, Johnson KR, Lakins JN, Rozenberg GI, Gefen A, Reinhart-King CA, Margulies SS, Dembo M, Boettiger D, Hammer DA, Weaver VM. 2005. Tensional homeostasis and the malignant phenotype. *Cancer Cell* 8(3):241–254.
- Patrick CW, Jr. 2000. Adipose tissue engineering: The future of breast and soft tissue reconstruction following tumor resection. *Semin Surg Oncol* 19(3):302–311.
- Pirone DM, Liu WF, Ruiz SA, Gao L, Raghavan S, Lemmon CA, Romer LH, Chen CS. 2006. An inhibitory role for FAK in regulating proliferation: A link between limited adhesion and RhoA-ROCK signaling. *J Cell Biol* 174(2):277–288.
- Rouillard AD, Tsui Y, Polachek WJ, Lee JY, Bonassar LJ, Kirby BJ. 2010. Control of the electromechanical properties of alginate hydrogels via ionic and covalent cross-linking and microparticle doping. *Biomacromolecules* 11(8): 2184–2189.
- Rouillard AD, Berglund CM, Lee JY, Polachek WJ, Tsui Y, Bonassar LJ, Kirby BJ. 2011. Methods for photocrosslinking alginate hydrogel scaffolds with high cell viability. *Tissue Eng Part C Methods* 17(2): 173–179.
- Rowley JA, Madlambayan G, Mooney DJ. 1999. Alginate hydrogels as synthetic extracellular matrix materials. *Biomaterials* 20(1): 45–53.
- Rubina K, Kalinina N, Efimenko A, Lopatina T, Melikhova V, Tsokolaeva Z, Sysoeva V, Tkachuk V, Parfyonova Y. 2009. Adipose stromal cells stimulate angiogenesis via promoting progenitor cell differentiation, secretion of angiogenic factors, and enhancing vessel maturation. *Tissue Eng Part A* 15(8):2039–2050.
- Samani A, Bishop J, Luginbuhl C, Plewes DB. 2003. Measuring the elastic modulus of ex vivo small tissue samples. *Phys Med Biol* 48(14):2183–2198.
- Sawhney AS, Pathak CP, Hubbell JA. 1993. Bioerodible hydrogels based on photopolymerized poly(ethylene glycol)-co-poly(alpha-hydroxy acid) diacrylate macromers. *Macromolecules* 26(4):581–587.
- Seib FP, Prewitz M, Werner C, Bornhauser M. 2009. Matrix elasticity regulates the secretory profile of human bone marrow-derived multipotent mesenchymal stromal cells (MSCs). *Biochem Biophys Res Commun* 389(4):663–667.
- Smeds KA, Pfister-Serres A, Miki D, Dastgheib K, Inoue M, Hatchell DL, Grinstaff MW. 2001. Photocrosslinkable polysaccharides for in situ hydrogel formation. *J Biomed Mater Res* 54(1):115–121.
- Stacey DH, Hanson SE, Lahvis G, Gutowski KA, Masters KS. 2009. In vitro adipogenic differentiation of preadipocytes varies with differentiation stimulus, culture dimensionality, and scaffold composition. *Tissue Eng Part A* 15(11):3389–3399.
- Subramanian A, Lin HY. 2005. Crosslinked chitosan: Its physical properties and the effects of matrix stiffness on chondrocyte cell morphology and proliferation. *J Biomed Mater Res A* 75(3):742–753.
- Taraboletti G, Roberts D, Liotta LA, Giavazzi R. 1990. Platelet thrombospondin modulates endothelial cell adhesion, motility, and growth: A potential angiogenesis regulatory factor. *J Cell Biol* 111(2):765–772.
- Ulrich TA, de Juan Pardo EM, Kumar S. 2009. The mechanical rigidity of the extracellular matrix regulates the structure, motility, and proliferation of glioma cells. *Cancer Res* 69(10):4167–4174.
- Underhill GH, Chen AA, Albrecht DR, Bhatia SN. 2007. Assessment of hepatocellular function within PEG hydrogels. *Biomaterials* 28(2):256–270.
- Wang N, Butler JP, Ingber DE. 1993. Mechanotransduction across the cell surface and through the cytoskeleton. *Science* 260(5111):1124–1127.
- Winer JP, Janmey PA, McCormick ME, Funaki M. 2009. Bone marrow-derived human mesenchymal stem cells become quiescent on soft substrates but remain responsive to chemical or mechanical stimuli. *Tissue Eng Part A* 15(1):147–154.
- Yoshida S, Ono M, Shono T, Izumi H, Ishibashi T, Suzuki H, Kuwano M. 1997. Involvement of interleukin-8, vascular endothelial growth factor, and basic fibroblast growth factor in tumor necrosis factor alpha-dependent angiogenesis. *Mol Cell Biol* 17(7):4015–4023.
- Zaman MH, Trapani LM, Sieminski AL, Mackellar D, Gong H, Kamm RD, Wells A, Lauffenburger DA, Matsudaira P. 2006. Migration of tumor cells in 3D matrices is governed by matrix stiffness along with cell–matrix adhesion and proteolysis. *Proc Natl Acad Sci USA* 103(29):10889–10894.